Environmental Pollution xxx (2017) 1–13

Contents lists available at ScienceDirect

Environmental Pollution

journal homepage: www.elsevier.com/locate/envpol

Ambient concentrations and deposition rates of selected reactive nitrogen species and their contribution to $PM_{2.5}$ aerosols at three locations with contrasting land use in southwest China☆

Ling Song [a, b], Xuejun Liu [c], Ute Skiba [d], Bo Zhu [a, b, *], Xifeng Zhang [a, b], Meiyu Liu [b], Marsailidh Twigg [d], Jianlin Shen [e], Anthony Dore [d], Stefan Reis [d], Mhairi Coyle [d], Wen Zhang [c], Peter Levy [d], David Fowler [d]

[a] Key Laboratory of Mountain Surface Processes and Ecological Regulation, Chinese Academy of Sciences, Chengdu, Sichuan 610041, China
[b] Institute of Mountain Hazards and Environment, Chinese Academy of Sciences, Chengdu, Sichuan 610041, China
[c] College of Resources and Environmental Sciences, China Agricultural University, Beijing 100193, China
[d] Centre for Ecology and Hydrology, Bush Estate, Penicuik, Midlothian EH26 0QB, UK
[e] Key Laboratory of Agro-Ecological Processes in Subtropical Regions, Institute of Subtropical Agriculture, Chinese Academy of Sciences, Changsha, Hunan 410125, China

ARTICLE INFO

Article history:
Received 3 April 2017
Received in revised form
28 September 2017
Accepted 1 October 2017
Available online xxx

Keywords:
Reduced nitrogen
Oxidized nitrogen
Seasonal pattern
Pollution source
Land use type

ABSTRACT

The fast economic development of southwest China has resulted in significant increases in the concentrations of reactive nitrogen (Nr) in the atmosphere. In this study, an urban (Chengdu, CD), suburban (Shifang, SF) and agriculture (Yanting, YT) – dominated location in the Sichuan Province, southwest China, were selected to investigate the atmospheric composition of Nr, their concentrations and deposition rates. We measured Nr concentrations in precipitation (NH_4^+, NO_3^- and organic N (DON)), the gas phase (NH_3 and NO_2), and the aerosol particles ($PM_{2.5}$), and calculated their fluxes over a two year period (2014–2016). Total annual N deposition rates were 49.2, 44.7 and 19.8 kg N ha^{-1} yr^{-1} at CD, SF and YT, respectively. Ammonia concentrations were larger at the urban and suburban sites than the agricultural site (12.2, 14.9, and 4.9 μg N m^{-3} at CD, SF and YT, respectively). This is consistent with the multitude of larger sources of NH_3, including city garbage, livestock and traffic, in the urban and suburban areas. Monthly NO_2 concentrations were lower in warmer compared to the colder months, but seasonal differences were insignificant. Daily $PM_{2.5}$ concentrations ranged from 7.7 to 236.0, 5.0–210.4 and 4.2–128.4 μg m^{-3} at CD, SF and YT, respectively, and showed significant correlations with fine particulate NH_4^+ and NO_3^- concentrations. Ratios of reduced to oxidized N were in the range of 1.6–2.7. This implies that the control of reduced Nr especially in urban environments is needed to improve local air quality.

1. Introduction

Global emissions of reactive forms of nitrogen (Nr) are increasing proportionally with the human population increase and had reached a total of 220 Tg N yr^{-1} in 2010 (Fowler et al., 2015). The dominant Nr species emitted to the atmosphere are ammonia (NH_3) and nitrogen oxides (NO_x), which are precursors of secondary aerosols, such as nitric acid (HNO_3), particulate NH_4^+ (pNH_4^+) and particulate NO_3^- (pNO_3^-) (Delon et al., 2012). Sources of NH_3 include agricultural activities (livestock and fertilizer use), mobile and stationary fuel combustion, industrial activities and biomass burning (Lee et al., 2016; Suarez-Bertoa et al., 2014). Nitrogen oxides (NO_x), which include NO_3^- in rainwater, gaseous NO_2 and HNO_3, and aerosol pNO_3^-, are mainly emitted from fossil fuel combustion and biomass burning (Zbieranowski and Aherne, 2013). These atmospheric Nr species are deposited to the Earth's surfaces via wet or dry deposition. Wet deposition occurs due to the incorporation of aerosol particles, acting as cloud condensation nuclei, into cloud droplets; as well as below-cloud and in-cloud scavenging of soluble gases. Dry deposition is primarily the deposition of gaseous compounds (NH_3, NO_2 and HNO_3), with aerosol

☆ This paper has been recommended for acceptance by Charles Wong.

* Corresponding author. No.9, Block 4, Renminnan Road, Chengdu, Sichuan, China.
E-mail address: bzhu@imde.ac.cn (B. Zhu).

https://doi.org/10.1016/j.envpol.2017.10.002
0269-7491/

making smaller contributions (Dore et al., 2015). Increased nitrogen (N) deposition rates have led to biodiversity reductions in terrestrial ecosystems (Stevens et al., 2004), damage to human health through aerosols and ozone production (Erisman et al., 2013) and indirectly contributing to the radiative forcing of our climate. With the rapid urbanization and industrialization in China, it was estimated that the current level of air pollution may have led to 400,000 premature deaths annually (Xu et al., 2016). The economic burden of this premature mortality is estimated at approximately 157 billion Yuan (1.16% of the GDP) (Zhang and Smith, 2007), and is of increasing concern for the general public, the environmental scientific community and policy makers.

Measures to reduce Nr emissions and deposition rates were successfully implemented in some countries. In Europe, for example, policies to reduce agriculture emissions (e.g. Common Agricultural Policy, Nitrates Directive and the restructuring of Eastern Europe after 1989) as well as stringent emission controls (e.g. EC Large Combustion Plants Directive) and the EUROPE standards for road transport vehicles were implemented in the 1980s (Sutton et al., 2007). As a result, in some European countries significant reductions in NH_3 volatilization has been achieved over the last 20 years (Sanz-Cobena et al., 2014). Similarly, the Chinese Government has implemented mitigation methods to reduce air pollution from stationary combustion plants in 2012. This mitigation was expected to reduce average Chinese annual NO_2 and $PM_{2.5}$ concentrations by 24.3% and 14.7%, respectively, by 2020 (Wang et al., 2015b). However, no regulations were implemented to reduce NH_3 emissions.

The Sichuan basin, located in the upper Yangtze River is an example of serious air pollution in China. Rapid population growth and economic expansion have resulted in a wide range of Nr producing anthropogenic activities, such as biomass and fossil fuel burning, industry, transport, mining, urbanization and agricultural activities. The Sichuan basin is one of the four largest regions affected by haze in China and is one of the world's region most polluted by $PM_{2.5}$ (Zhang et al., 2012). In addition, large emissions of SO_2 and NO_x have decreased the precipitation pH (Vet et al., 2014). Although the serious air pollution problems in the Sichuan basin are recognized, scientific evidence has focused mainly on wet deposition (Liu et al., 2013). More recent studies have shown that dry deposition rates can be large (Xu et al., 2015). As it is important to investigate wet and dry deposition rates together, we have investigated these at an urban, suburban and agricultural location. Our aims were to quantify 1) seasonal and spatial patterns for Nr concentrations and ambient $PM_{2.5}$ concentrations; 2) the proportion of reduced and oxidized N deposition; and 3) the contribution of Nr species to ambient $PM_{2.5}$ concentration.

2. Materials and methods

2.1. Sampling sites

Nitrogen deposition measurements were conducted at Chengdu (CD, 30°37′ N, 104°4′ E), Shifang (SF, 31°6′ N, 104°9′ E) and Yanting (YT, 30°21′ N, 105°12′ E), Sichuan Province, southwest China. These three locations represent urban, suburban and agricultural areas, respectively (Fig. 1). Nr bulk deposition of NH_4^+, NO_3^- and organic N (DON), dry deposition of the gas phase (NH_3 and NO_2) and the aerosol particles ($PM_{2.5}$) were measured during the period January 2014 to April 2016. All compounds were measured at all three locations continuously for at least one year (Table S1), but started and ended at slightly different times. The time period when all compounds and locations were measured at three locations was over an 8 month period, May to December 2015.

The study region has a moderate subtropical monsoon climate with an annual mean temperature of 17.3 °C and a mean annual precipitation of 826 mm for the period 1981–2015. The precipitation distribution has a seasonal character, and is larger in summer than in winter. Due to it's topographic, Sichuan has the lowest wind speeds in China according to Sichuan Muni CIPAL Bureau of Statistics, 2015 and thereby favors the accumulation of atmospheric pollutants. The main meteorological characteristics are shown in Fig. 1. The urban measurement site CD (Chengdu) is located in the city center close to a major ring road. Chengdu is the capital of Sichuan province with a population of about 12 million and surrounded by the Longquan Mountains to the east and Qionglai Mountains to the west. The suburban site SF is located within in the Chengdu Plain Agricultural Ecology Research Station, Chinese Academy of Sciences and about 50 km northeast of CD city center. It has a population of about 0.43 million. The agricultural measurement station YT is a typical agriculture dominated site near Yanting town, Mianyang city and about 150 km away from Chengdu city center (Fig. 1). It has a population of about 0.62 million. The main crops are maize, wheat and oil rape at both urban and suburban site (Zhu et al., 2009).

2.2. Collection and analysis of bulk deposition samples

All three monitoring sites are equipped with the widely used "standard rain gauge" (SDM6, Tianjin Weather Equipment Inc., China), which are situated within the grounds of CAS research stations and free from nearby obstacles. The continuously open collectors collect the bulk deposition, which includes both in-cloud and below-cloud scavenging as well as a small contribution of dry deposited aerosols and gases and thereby may overestimate the actual wet deposition (Cape and Leith, 2002). To minimize the accumulation of dry deposited material onto the funnel walls, collection vessels were cleaned with deionized water daily when there was rain, and every second day when there was no rain. The bulk deposition collected therefore only includes a very small proportion of the actual dry deposition.

The method to collect bulk deposition is based on the method recommended by the European Monitoring and Evaluation Program (EMEP) and described in detail by Aas et al. (2007). Collectors consist of a glass measuring cylinder (scale range: 0–10 mm, division: 0.1 mm) set within each rain gauge. Collectors are checked daily around 8 a.m., and any rainfall accumulated over the previous 24 h was collected then to minimize inputs from dry deposition and evaporation. The rain samples were transferred to clean polyethylene bottles within 24 h of each rain event, and stored in a freezer at −20 °C until chemical analysis within one month. The bottles were first soaked in HCl (2%) overnight and then cleaned with deionized water. All procedures were strictly quality-controlled to avoid any possible contamination of the samples. Before analysis, samples were defrosted and then filtered through a 0.45-μm membrane filter. Ammonium (NH_4^+) and nitrate (NO_3^-) concentrations were analyzed by a flow injection auto-analyzer (Bran + Lubbe, Norderstedt, Germany). Precipitation samples were analyzed in duplicates. One blank and a set of standard concentrations of NH_4-N, NO_3-N and TDN were analyzed after every 10 samples. Standard solutions were prepared in ultrapure water (18.2 MΩ resistance) with concentrations ranges of 0–7, 0–7 and 0–20 mg l^{-1} for NH_4-N, NO_3-N and TDN, respectively. The detection limit was 0.01 mg N l^{-1} for both NH_4^+ and NO_3^- concentrations. Since NO_3^- was converted to NO_2^- during the chemical analysis, the measured NO_3^- concentration is the sum of NO_3^- and NO_2^- in rainwater. The total dissolved N (TDN) content in the filtrate was measured using the alkaline potassium persulfate oxidation method, and has a detection limit of 0.01 mg N l^{-1} (Rowland and Haygarth, 1997). Dissolved organic N (DON) concentrations were

Please cite this article in press as: Song, L., et al., Ambient concentrations and deposition rates of selected reactive nitrogen species and their contribution to $PM_{2.5}$ aerosols at three locations with contrasting land use in southwest China, Environmental Pollution (2017), https://doi.org/10.1016/j.envpol.2017.10.002

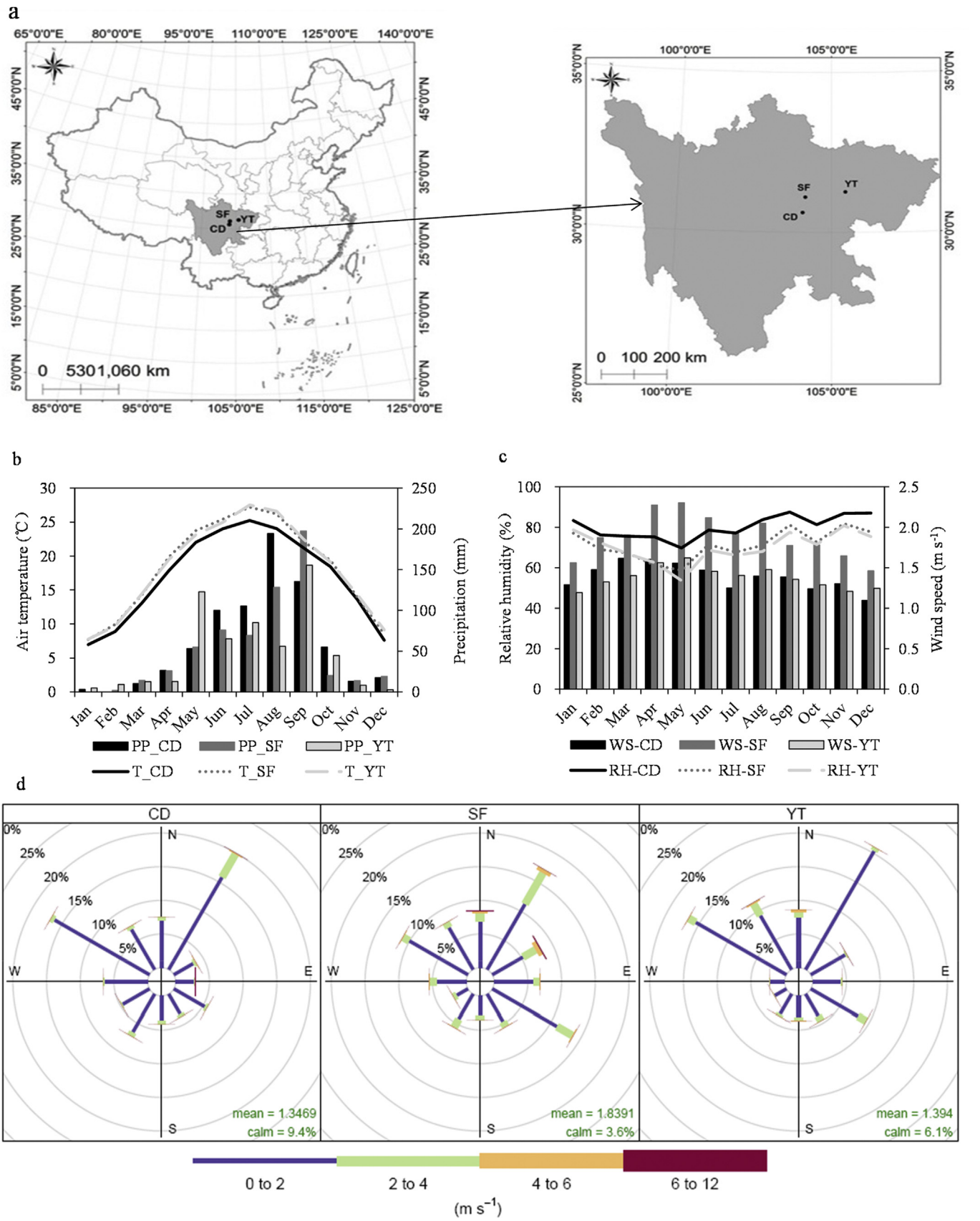

Fig. 1. Description for the deposition monitoring sites: a) location of the three sampling sites (CD, SF and YT) in Sichuan province, Southwest China, b) mean monthly precipitation (PP) and air temperature (T), c) monthly mean relative humidity (RH) and wind speed (WS), d) wind rose of 3-h wind directions (WD) and wind speeds during the study period 2014–2016 at the three study sites.

Please cite this article in press as: Song, L., et al., Ambient concentrations and deposition rates of selected reactive nitrogen species and their contribution to $PM_{2.5}$ aerosols at three locations with contrasting land use in southwest China, Environmental Pollution (2017), https://doi.org/10.1016/j.envpol.2017.10.002

calculated from the difference of TDN and inorganic N concentrations (Bronk et al., 2000). Therefore the detection limit of DON is assumed to be the sum of the detection limits of the TDN + NH_4^+ + NO_3^-, 0.03 mg N l^{-1}.

2.3. Collection and analysis of gaseous Nr samples

Ammonia (NH_3) concentrations were measured using ALPHA (Adapted Low-cost Passive High Absorption) samplers. These are passive samplers provided by the Center for Ecology and Hydrology, UK (Tang et al., 2001), and are widely used in several national motoring networks, as they are reliable, accurate, cost effective and easy to use (Puchalski et al., 2011). Each sampler consists of a 26 mm long × 27 mm outer diameter polyethylene tube. One end contains a 5 μm PTFE membrane through which NH_3 gas diffuses, but not particles. Ammonia is absorbed onto a filter impregnated with citric acid (13%) located at the other end of the diffusion path. Inter-comparison of the passive ALPHA samplers with active DELTA samplers (DEnuder for Long-Term Atmospheric sampling) showed a high agreement between these methods (Tang et al., 2001; Xu et al., 2015). Field blank measurements were made seasonally at all study sites, and the variability between triplicate alpha samplers was approximately 7%.

Nitrogen dioxide (NO_2) was collected using Gradko diffusion tubes (Gradko International Limited, UK). These passive samplers are used very widely (Ozden and Dogeroglu, 2008), for example in the UK NO_2 Monitoring Network (Tang et al., 2001). Each sampler consists of a 71 mm long × 11 mm internal diameter acrylic tube with colored and white thermoplastic rubber caps. The NO_2 is absorbed by a 20% triethanolamine/deionized water solution coated onto two stainless steel wire meshes within the colored cap. The manufacturer Gradko International Ltd, UK specifies a NO_2 uptake rate of 68.8 × 10^{-6} m^{-3} h^{-1}, a desorption efficiency of 0.98, a limit of detection of 1.6 μg NO_2 m^{-3} over a 2-week exposure period, and an analytical measurement uncertainty of ±10%. A comparison with a chemiluminescent instrument indicates no significant difference in the performance of both methods (Bush et al., 2001). Field blank measurements (n = 3) were made seasonally at all study sites. The standard deviations of all samples across all sites and the entire measurement period ranged from 0.01 to 2.9 μg NO_2 m^{-3} and averaged at 0.8 μg NO_2 m^{-3} (95% confidence interval 0.7–0.9).

At all three study sites three NH_3 and NO_2 samplers were exposed under a PVC shelter which protected the samplers from precipitation and direct sunshine over the one month measurement period. After collection samples were stored at 4 °C and analyzed within one month of collection. NH_3 was extracted in 10 ml ultrapure water, and extracts were stored at 4 °C prior to analysis using a flow injection auto-analyzer (Bran + Lubbe, Norderstedt, Germany). The detection limit for NH_3 was 0.01 mg N L^{-1}. NO_2 was extracted with sulfanilamide, H_3PO_4, and N-1-naphthylene-diamine, and determined using a colorimetric method at a wavelength of 542 nm. The detection limit for NO_2 was 0.01 mg N L^{-1} (Xu et al., 2015).

2.4. Collection and analysis of $PM_{2.5}$ samples

Samples for $PM_{2.5}$ analysis were collected onto 90-mm diameter quartz fiber filters (Whatman QM/A, Maidstone, UK) using medium-volume samplers (TH-150 CIII, 100 L min^{-1}, Tianhong Co., Wuhan, China) at all the three sites. The quartz fiber filters were baked at 500 °C for 4 h prior to exposure to remove contaminants. $PM_{2.5}$ samples were collected after 24 h exposure from 8:00 a.m. to 8:00 a.m. the next day. Sample frequency was every three days. Zhang et al. (2017) have demonstrated that the integration to monthly or annual values from daily samples compared to a sample taken only every three days was very similar. Before and after sampling, the filters were equilibrated for 24 h in a desiccator at 25 °C and 40% relative humidity and then weighted using a microbalance (Sartorius, precision 10 μg). Then, filters were stored in clean tubes at 4 °C until analyzing within 1 month. The $PM_{2.5}$ concentrations were calculated by weight differences divided by the flow rate. Half of each filter was placed into a 50 ml breaker with 20 ml of ultrapure water, the second half of the filter was stored at 4 °C in case the analysis had to be repeated. After a 30-min ultrasonic extraction, the extracts were filtered using 0.22 μm quartz syringe filters. Cations (NH_4^+, Na^+, Ca^{2+}, K^+, Mg^{2+}) and anions (NO_3^-, SO_4^{2-}, F^-, Cl^-) in the filtrates were determined using a Dionex-600 and Diones-2100 Ion Chromatograph (Diones Inc., Sunnyvale, CA, USA), respectively (Ianniello et al., 2011; Zhao et al., 2013). Three blank filters were included in the analysis of each set of samples, following the same procedures as for the analysis of the water-soluble inorganic ions. To calculate the actual concentrations, blank concentrations were subtracted from the sample concentrations. We tested the validity of using only one half of the filter for the analysis by weighing and analyzing both halves for a subset of filters. Differences in weight and concentrations were negligible.

2.5. Deposition calculation

As in previous studies (Liu et al., 2013), the bulk N deposition rate was calculated as the product of the precipitation amount and the concentration of Nr species in rainwater. The monthly or annual bulk deposition rate (BDR) of Nr species can be expressed using the following equation:

$$\text{Monthly}\left(\text{kg N ha}^{-1}\ \text{month}^{-1}\right)\ \text{or}\ \text{annual}\left(\text{kg N ha}^{-1}\ \text{yr}^{-1}\right)\text{BDR} = 0.01\sum_{i=1}^{n} C_i P_i$$

where 'C' is the measured concentration of N in rainwater (mg N l^{-1}); 'P' is the rainwater amount of an individual precipitation event (mm); 'n' is the number of precipitation events at the corresponding monthly or annually scale; and '$_i$' is the count of precipitation events. Then, the monthly or yearly N volume-weighted concentrations (VWC) of N species were calculated using the following equation:

$$\text{Monthly or annual VWC}\ \left(\text{mg N l}^{-1}\right) = 100 \times \text{BDR}/\sum_{i=1}^{n} P_i$$

The Nr dry deposition rates were estimated by the inferential technique, which combines measured concentrations of Nr species and their deposition velocities. According to Flechard et al. (2011), the dry deposition rate of each Nr species (F) can be expressed as:

$$F = C_{Nr} \times V_d$$

where 'C_{Nr}' is the measured concentration of individual Nr species, μg N m^{-3}; 'V_d' is the deposition velocity (cm s^{-1}). As the V_d was not measured in this study, it was calculated using a well-tested V_d model together with empirical parameters from the literature and meteorological data from the three study locations (Petroff and Zhang, 2010; Wesely and Hicks, 1977; Zhang et al., 2001). Details

Please cite this article in press as: Song, L., et al., Ambient concentrations and deposition rates of selected reactive nitrogen species and their contribution to $PM_{2.5}$ aerosols at three locations with contrasting land use in southwest China, Environmental Pollution (2017), https://doi.org/10.1016/j.envpol.2017.10.002

of the calculations and model parameters are described byKuang et al. (2016) and Shen et al. (2016). The modeled mean dry deposition velocities for NH_3, NO_2, pNH_4^+ and pNO_3^- were 0.27, 0.03, 0.24 and 0.24 cm s^{-1} at CD, and 0.23, 0.10, 0.19 and 0.19 cm s^{-1} at SF and YT, respectively.

2.6. $PM_{2.5}$ concentration and variability with wind direction

The polar plots and frequency distribution plots for $PM_{2.5}$ concentrations were calculated based on daily $PM_{2.5}$ concentrations combined with the meteorological data using the Openair software (Carslaw and Ropkins, 2012). Meteorological data for Fig. 1b and c are average values for each month during the monitoring period. Data for temperature (T), relative humidity (RH), wind speed (WS) and wind direction (WD) were downloaded from https://rp5.ru/. Wind rose maps (Fig. 1d) were produced using R language (R Development Core Team, 2011). Descriptive statistical and Pearson correlation analyses were performed using the SPSS software package, version 14.0 (SPSS Inc., Chicago, IL). When conducting the Pearson correlation and linear regression analyses, significance was evaluated using a significance level (p) of 0.05.

3. Results

3.1. Concentrations of Nr species in rainwater

The monthly concentrations of NH_4^+, NO_3^- and DON in rainwater at the three study sites are shown in Fig. 2. Here we classify the periods of March–May, June–August, September–November and January, February and December as spring, summer, autumn and winter. At CD, both NH_4^+ and NO_3^- concentrations in winter (5.4 ± 0.8 mg N l^{-1} for NH_4^+; 10.7 ± 2.8 mg N l^{-1} for NO_3^-) were significantly higher than in the other seasons ($p < 0.05$). The highest and lowest DON concentrations were measured in the spring (1.6 ± 1.4 mg N l^{-1}) and autumn (0.4 ± 0.1 mg N l^{-1}), but differences between the seasons were not significant (Fig. 2a). Similarly at SF, NH_4^+ (8.3 ± 0.3 mg N l^{-1}) and NO_3^- (3.5 ± 0.2 mg N l^{-1}) concentrations were significantly higher ($p < 0.05$) in winter compared to other seasons, and autumn and spring had significantly higher concentrations than in summer ($p < 0.05$). DON concentrations were lower in autumn and higher in winter, but there were no significant ($p > 0.05$) seasonal difference (Fig. 2b). At YT average winter concentrations of NH_4^+, NO_3^- and DON were 2.8 ± 0.9, 2.8 ± 0.3 and 1.5 ± 0.8 mg N l^{-1}, respectively, and were significantly higher than in the other seasons. Differences between spring, summer and autumn seasons were not significant for all three N forms (Fig. 2c). Comparing monthly concentrations showed that all three N forms were significantly higher in the dry months (January (CD), November (SF) and February (YT)), and significantly lower in the wet months (August (CD and YT) and July (YT)). Comparison by site showed that the highest annual NH_4^+ and NO_3^- concentrations were found in SF and CD, respectively, while the highest DON concentration was found in YT.

3.2. Concentrations of gaseous and particulate Nr

Annual NH_3 concentrations at CD (12.2 ± 2.8 μg N m^{-3}) and SF (14.9 ± 4.5 μg N m^{-3}) were significantly higher ($p < 0.01$) than at YT (4.9 ± 4.9 μg N m^{-3}), but there were no statistical significant differences between CD and YT (Fig. 3a). Looking at seasonal variations, average NH_3 concentrations at all three locations were significantly higher ($p < 0.01$) in summer (14.1 ± 0.6, 17.7 ± 0.9 and 10.0 ± 8.1 μg N m^{-3} at CD, SF and YT, respectively) than in winter (9.5 ± 0.4, 10.6 ± 1.4 and 1.9 ± 1.5 μg N m^{-3} at CD, SF and YT, respectively). At the monthly scale, NH_3 concentrations were

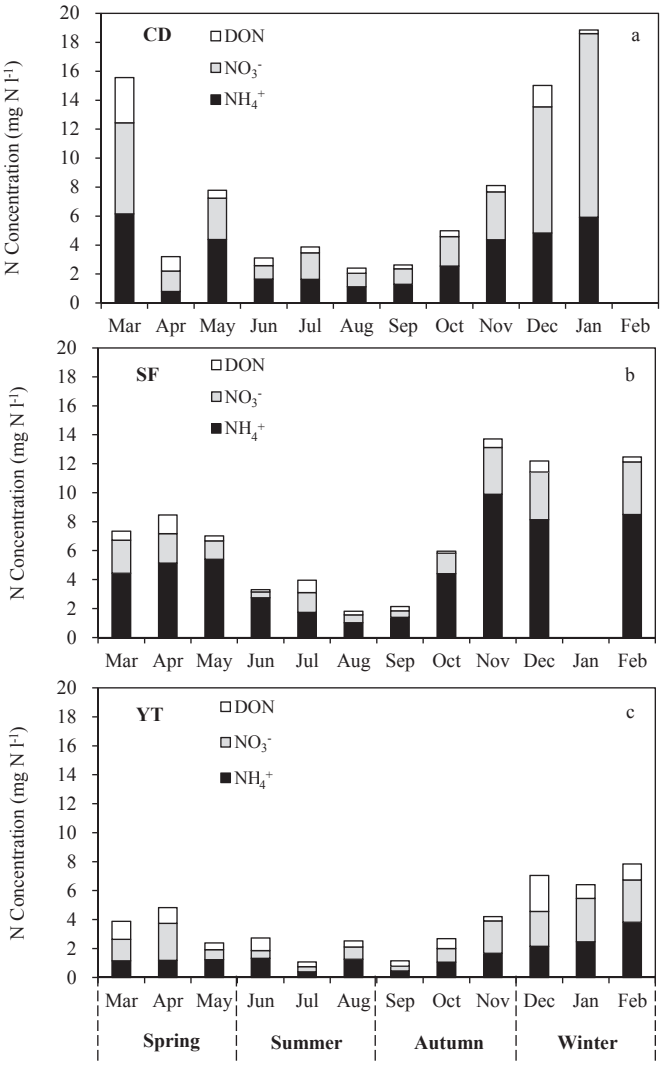

Fig. 2. Monthly volume-weighted mean concentrations of NH_4^+, NO_3^- and DON in rainwater at CD (a), SF (b) and YT (c). There was no precipitation at CD in February and at SF in January.

significantly higher in June at SF (23.2 ± 0.9 μg N m^{-3}) and in July in YT (18.8 ± 0.4 μg N m^{-3}) compared to the other months ($p < 0.01$).

Annual NO_2 concentrations were highest in CD (15.4 ± 2.8 μg N m^{-3}), followed by SF (10.6 ± 1.9 μg N m^{-3}), and lowest in YT (2.6 ± 1.1 μg N m^{-3}). The differences between the three monitoring sites were significant ($p < 0.01$) (Fig. 3b). At CD, the highest monthly NO_2 concentration measured in December (19.5 ± 2.6 μg N m^{-3}) was two times larger than the lowest concentration in May (9.6 ± 1.7 μg N m^{-3}). At SF, the highest and lowest NO_2 concentrations were observed in November (13.6 ± 1.9 μg N m^{-3}) and May (8.1 ± 1.6 μg N m^{-3}), respectively. At the YT site, the highest and lowest NO_2 concentrations were found in October (4.0 ± 0.02 μg N m^{-3}) and July (0.4 ± 0.3 μg N m^{-3}), respectively.

Average daily concentrations of fine particulate NH_4^+ (pNH_4^+) throughout the monitoring period were 5.9 ± 3.1, 5.1 ± 2.2, and 3.0 ± 1.5 μg N m^{-3} at CD, SF and YT, respectively (Fig. 3c). In winter pNH_4^+ concentrations (10.6 ± 0.7, 8.1 ± 0.8 and 4.7 ± 1.8 μg N m^{-3} at CD, SF, and YT, respectively) were significantly higher ($p < 0.05$) than in the remaining seasons. The highest pNH_4^+ concentrations occurred in the dry, cold months of January (at CD and SF) and February (at YT). The lowest pNH_4^+ concentrations occurred in

Please cite this article in press as: Song, L., et al., Ambient concentrations and deposition rates of selected reactive nitrogen species and their contribution to $PM_{2.5}$ aerosols at three locations with contrasting land use in southwest China, Environmental Pollution (2017), https://doi.org/10.1016/j.envpol.2017.10.002

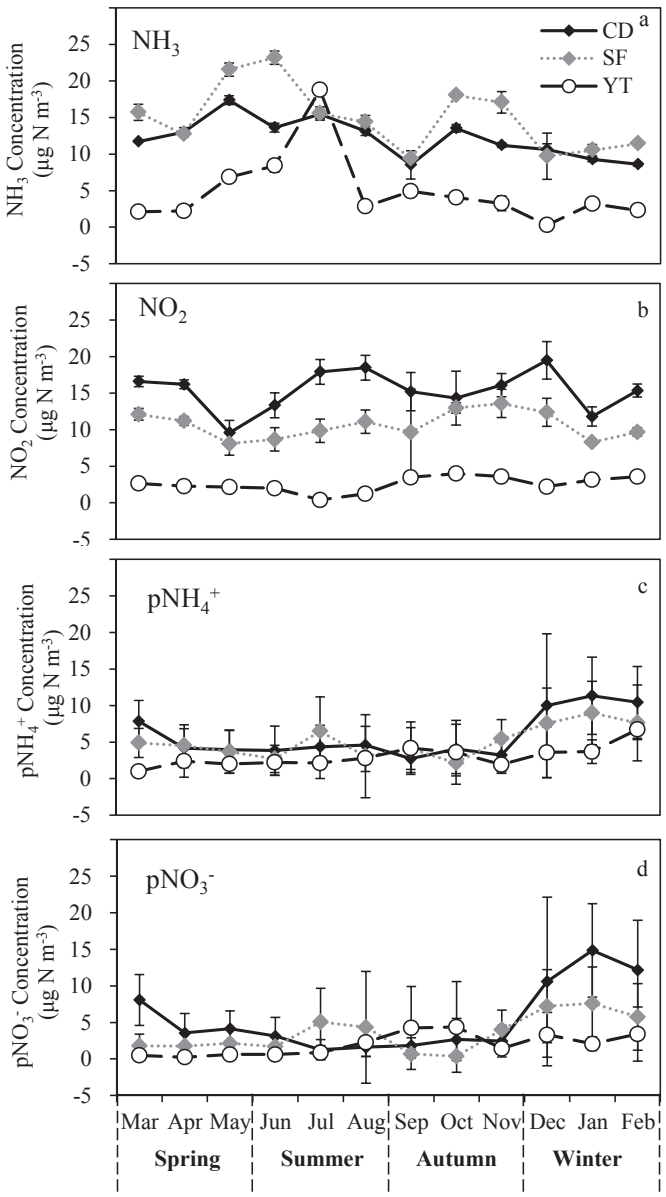

Fig. 3. Monthly gaseous N (NH_3 (a) and NO_2 (b)) and aerosol N (pNH_4^+ (c) and pNO_3^- (d)) concentrations at CD, SF and YT during the monitoring period. Data for pNH_4^+ and pNO_3^- were average values of the daily results within each month. Data were shown as the monthly average values ± standard deviation. Some of the segments are not visible because the small uncertainty.

September at CD, in October at SF, and in March at YT.

Average daily concentrations of fine particulate NO_3^- (pNO_3^-) were 5.5 ± 4.7, 3.5 ± 2.5 and 2.0 ± 1.5 μg N m^{-3} at CD, SF and YT, respectively (Fig. 3d). At CD, pNO_3^- concentrations in winter (12.5 ± 2.2 μg N m^{-3}) were significantly higher ($p < 0.05$) than in the remaining seasons. Similarly highest pNO_3^- concentrations at SF were also measured in winter (6.9 ± 1.0 μg N m^{-3}), when pNO_3^- concentrations were significantly higher ($p < 0.05$) than in spring (1.9 ± 0.2 μg N m^{-3}) and autumn (1.7 ± 1.4 μg N m^{-3}), but not significantly ($p > 0.05$) different from summer concentrations (3.7 ± 3.2 μg N m^{-3}). At YT, pNO_3^- concentrations in autumn (3.4 ± 1.7 μg N m^{-3}) and winter (2.9 ± 0.8 μg N m^{-3}) were significantly higher ($p < 0.05$) than in spring (0.5 ± 0.2 μg N m^{-3}) and summer (1.3 ± 0.9 μg N m^{-3}). Comparing monthly variability, highest pNO_3^- concentrations were found in January at CD and SF, and in September at YT, whereas lowest pNO_3^- concentrations were measured in July at CD, in October at SF, and in April at YT.

3.3. Ambient concentrations and chemical components of $PM_{2.5}$

The summary statistics for daily average $PM_{2.5}$ concentrations during the study period at the three sites are shown in Table 1. The $PM_{2.5}$ concentrations were in the range of 7.7–236.0, 5.0–210.4 and 4.2–128.4 μg m^{-3} at CD, SF and YT, respectively. Daily average $PM_{2.5}$ concentrations at CD (83.6 ± 40.8 μg m^{-3}) were significantly higher ($p < 0.05$) than at YT (41.5 ± 222.2 μg m^{-3}), while there was no significant difference with SF (69.2 ± 35.7 μg m^{-3}). $PM_{2.5}$ concentrations had similar seasonal distributions at all three study sites (Fig. 4). In winter $PM_{2.5}$ concentrations (119.0 ± 17.5, 92.9 ± 8.8 and 73.1 ± 20.3 μg m^{-3} at CD, SF and YT, respectively) were significantly higher ($p < 0.05$) than in summer (57.5 ± 4.1, 41.5 ± 4.0 and 30.1 ± 3.7 μg m^{-3} at CD, SF and YT, respectively) and autumn (69.2 ± 15.4, 57.4 ± 20.2 and 34.2 ± 6.9 μg m^{-3} at CD, SF and YT, respectively), but no significant differences ($p > 0.05$) were observed in spring (86.8 ± 15.9, 66.3 ± 4.7 and 50.6 ± 9.2 μg m^{-3} at CD, SF and YT, respectively). However, $PM_{2.5}$ concentrations in spring were significantly higher than in summer ($p < 0.05$) at all three study sites. Highest concentrations of $PM_{2.5}$ were found in January at CD and SF, which were about 2.4 and 3 times higher than the lowest concentrations in July at CD and in September at SF. At YT highest $PM_{2.5}$ concentration was measured in February. This concentration was about 3.7 times higher than the lowest concentration in August.

Proportions of water-soluble inorganic ions in $PM_{2.5}$ were 28.6%, 32.9% and 32.4% at CD, SF and YT, respectively. Secondary inorganic aerosols (NH_4^+, NO_3^- and SO_4^{2-}) were the dominant water-soluble inorganic ions and accounted for 24.5%, 29.1% and 26.6% of the

Table 1
Summary of daily average $PM_{2.5}$ concentrations (μg m^{-3}) and inorganic ionic species concentrations at the urban site (CD), the suburban site (SF) and the agricultural site (YT).

	CD	SF	YT
Daily average $PM_{2.5}$ concentrations			
$PM_{2.5}$ (μg/m^3)	83.6	69.2	41.5
Median	73.4	61.8	38.4
Min	7.7	5.0	4.2
Max	236.0	210.4	128.4
SD	40.8	35.7	22.2
n[a]	210	143	190
ECGS(%)[b]	49.5	35.0	8.2
EWHOS(%)[c]	97.1	95.1	75.3
Inorganic ionic species concentrations in $PM_{2.5}$			
SO_4^{2-} (μg/m^3)	11.7 ± 8.1[d]	10.7 ± 7.4	6.7 ± 5.1
NH_4^+(μg/m^3)	5.6 ± 5.3	5.6 ± 4.3	3.0 ± 3.1
NO_3^- (μg/m^3)	5.1 ± 6.5	4.1 ± 4.7	2.3 ± 4.4
Na^+ (μg/m^3)	1.2 ± 0.6	1.1 ± 0.3	1.2 ± 1.3
K^+ (μg/m^3)	1.1 ± 0.9	1.0 ± 0.7	0.9 ± 1.3
Ca^{2+} (μg/m^3)	1.2 ± 0.7	0.5 ± 1.0	0.6 ± 0.5
Mg^{2+} (μg/m^3)	0.6 ± 1.1	0.7 ± 1.0	0.4 ± 0.5
Cl^- (μg/m^3)	0.3 ± 0.8	0.3 ± 0.6	0.2 ± 0.4
F^- (μg/m^3)	2.1 ± 3.6	0.4 ± 1.1	0.1 ± 0.1
Sum of inorganic ionic species (μg/m^3)	23.9 ± 13.9	22.8 ± 12.3	13.4 ± 9.6
Secondary inorganic aerosol (μg/m^3)	20.5 ± 12.9	20.1 ± 12.0	11.0 ± 9.3
WSII(%)[e]	28.6 ± 16.6	32.9 ± 17.8	32.4 ± 23.2
SIA(%)[f]	24.5 ± 15.5	29.1 ± 17.3	26.6 ± 22.4

[a] "n" is the number of samples.
[b] Proportion of sampling days when $PM_{2.5}$ concentrations exceeded the Chinese Grade II standard.
[c] Proportion of sampling days when $PM_{2.5}$ concentrations exceeded the WHO standard.
[d] Concentrations are average values ± standard deviation during the study period.
[e] Proportion of water-soluble inorganic ions in $PM_{2.5}$.
[f] Proportion of secondary inorganic aerosol (SIA) in $PM_{2.5}$.

Please cite this article in press as: Song, L., et al., Ambient concentrations and deposition rates of selected reactive nitrogen species and their contribution to $PM_{2.5}$ aerosols at three locations with contrasting land use in southwest China, Environmental Pollution (2017), https://doi.org/10.1016/j.envpol.2017.10.002

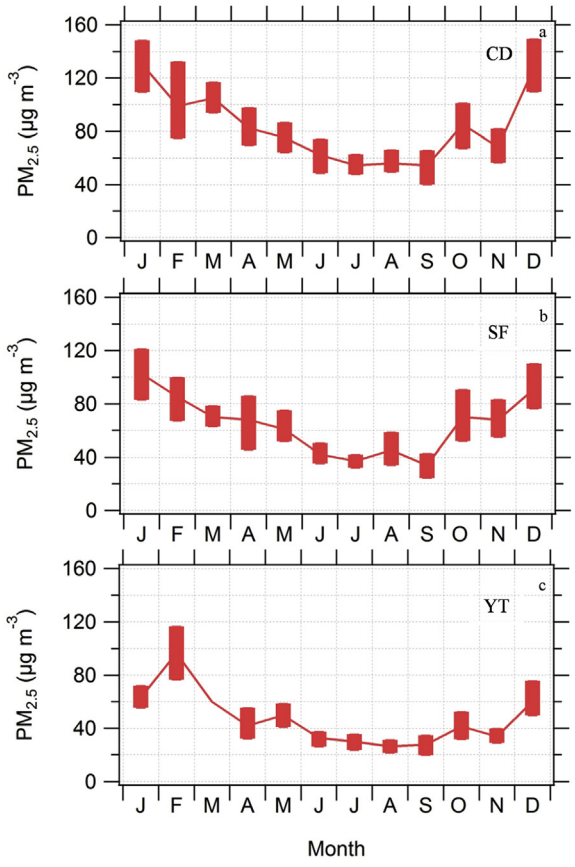

Fig. 4. Monthly averaged ambient $PM_{2.5}$ concentrations at CD (a), SF (b) and YT (c). Data were based on the daily results for each month within the study period. The line is the mean value and the shaded area is the 95% confidence of the monthly mean. (Graphs produced using Openair; Carslaw and Ropkins, 2012).

$PM_{2.5}$ concentration at CD, SF and YT, respectively. The magnitude of concentrations were in the following order: $SO_4^{2-} > NH_4^+ > NO_3^- > Na^+ > K^+ > Ca^{2+} > Mg^{2+} > F^- > Cl^-$, except that the concentration of Ca^{2+} was higher than K^+ at CD, and Cl^- was higher than F^- at YT. Sulphate was the dominant water-soluble inorganic ions in $PM_{2.5}$ at all three sites and increased in the following order: agricultural < suburban < urban. Compared to the secondary inorganic aerosols, Na^+, K^+, Ca^{2+}, Mg^{2+}, Cl^- and F^- constituted a minor fraction (4–6%) of the water-soluble inorganic ions in $PM_{2.5}$ (Table 1).

3.4. Nr species deposition rates

Annual deposition rates of reduced N, which includes NH_4^+ in rainwater, gaseous NH_3 and aerosol pNH_4^+, were significantly higher at CD (28.1 kg N ha^{-1} yr^{-1}) and SF (29.2 kg N ha^{-1} yr^{-1}) than at YT (10.7 kg N ha^{-1} yr^{-1}). The deposition rates of reduced N in winter (5.0, 4.1 and 1.1 kg N ha^{-1} yr^{-1}, respectively, at CD, SF and YT) were significantly lower ($p < 0.01$) than in other seasons at all three sites (Fig. 5a). The contributions of NH_4^+ in rainwater to the total reduced N deposition in winter were significantly lower ($p < 0.01$) than in other seasons, whereas the contribution of gaseous NH_3 and aerosol pNH_4^+ to reduced N total deposition were significantly higher ($p < 0.01$) in winter. The annual deposition rates for oxidized N was highest in CD (17.7 kg N ha^{-1} yr^{-1}), followed by SF (10.6 kg N ha^{-1} yr^{-1}), and lowest in YT (6.1 kg N ha^{-1} yr^{-1}). The differences between the three sites were significant ($p < 0.01$) (Fig. 5b). The contribution of NO_3^- in rainwater to oxidized N total deposition in winter was significantly lower than in the other seasons. The annual deposition rates of DON in rainwater showed significantly higher ($p < 0.01$) deposition rates in summer and significantly lower ($p < 0.01$) deposition rates in winter (Fig. 5c). The average contributions of DON to bulk N deposition at YT (23.3 ± 4.5%) was significantly higher ($p < 0.01$) than in CD (11.1 ± 2.9%), but not significantly ($p > 0.05$) different to that of SF (15.3 ± 11.8%) ($p > 0.05$) (Fig. 5d). The annual N bulk deposition rates of NH_4^+, NO_3^- and DON were in the range of 5.5–13.5, 4.1–12.1 and 3.1–3.4 kg N ha^{-1} yr^{-1}, respectively. And the annual dry deposition rates of NH_3, NO_2, pNH_4^+ and pNO_3^- were in the range of 3.5–10.7, 0.8–3.3, 1.6–4.4 and 1.1–4.1 kg N ha^{-1} yr^{-1}, respectively. The annual total N deposition (bulk plus dry deposition) rates were 49.2, 44.7 and 19.8 kg N ha^{-1} yr^{-1} at CD, SF and YT, respectively, with relatively higher N deposition in summer and lower N deposition in winter through all of the three study sites (Fig. 5e).

4. Discussion

4.1. Nr species concentration

Atmospheric wet deposition includes (1) rainout: within-cloud scavenging where aerosol-type air pollutants that can be transported over long distances-up to 1000 km are incorporated in cloud droplets which finally precipitate as rain, and (2) washout: below-cloud scavenging of dust and gases often occurs close to the emitting source (Zimmermann et al., 2003). As a result, seasonal patterns of NH_4^+ and NO_3^- concentrations in rainwater are strongly influenced by precipitation amount (Huang et al., 2015). In the present study, NH_4^+ and NO_3^- in rainwater showed significantly lower concentrations in the rainy summer and higher concentrations in the dry winter. The monsoon climate determined the precipitation distribution pattern (Fig. 1). In addition, the low mixing height and low temperature in winter also contributed to this seasonal variation (Wang et al., 2016). For example, in the warmer seasons warm and hot temperatures evaporate NO_3^- back to HNO_3, the latter can then be dry deposited faster and be removed from the atmosphere (Zhang et al., 2008). Lower air temperatures favor the formation of NH_4NO_3 and increase the concentrations of both NH_4^+ and NO_3^- under the condition of abundant NH_3 for fully neutralizing SO_4^{2-} (Squizzato et al., 2013). At all our three study sites, rainwater NH_4^+ concentrations were significantly higher than those collected at deposition hotspots such as India (0.2–0.4 mg N l^{-1} for NH_4^+; 2.5–11.2 mg N l^{-1} for NO_3^-), whereas NO_3^- concentrations in rainwater were comparable to those in India (Bisht et al., 2017).

Previous studies have shown that sources of atmospheric NH_3 concentrations are dominated by agricultural activities (Fowler et al., 2015). This was also the case at the agricultural (YT) and suburban (SF) sites. Largest monthly NH_3 concentrations were observed in June or July when N fertilizer was applied to the crops, which is predominately maize at both YT and SF. Interestingly, average NH_3 concentrations at the urban (CD) and suburban (SF) sites were significantly higher ($p < 0.01$) than at the agricultural site (YT). This was also observed by Meng et al. (2011) comparing an urbanized and more rural location in Bejing, and by Wang et al. (2015a). One explanation for the larger urban and suburban NH_3 concentrations is the multitude of sources, human sewage, garbage, traffic and also a relatively large number of livestock (Meng et al., 2011; Sutton et al., 2000). In Sichuan province, NH_3 emitted from livestock production (619.8 × 10^3 t) is about 2.7 times larger than from fertilizer application (230.2 × 10^3 t). Together these two sources contribute with 85% to the total NH_3 emissions (Feng et al., 2015). The Chengdu statistic yearbook (2015 and 2016) lists NH_3 emissions to be the highest (101.1 × 10^3 t) in the Sichuan province.

Please cite this article in press as: Song, L., et al., Ambient concentrations and deposition rates of selected reactive nitrogen species and their contribution to $PM_{2.5}$ aerosols at three locations with contrasting land use in southwest China, Environmental Pollution (2017), https://doi.org/10.1016/j.envpol.2017.10.002

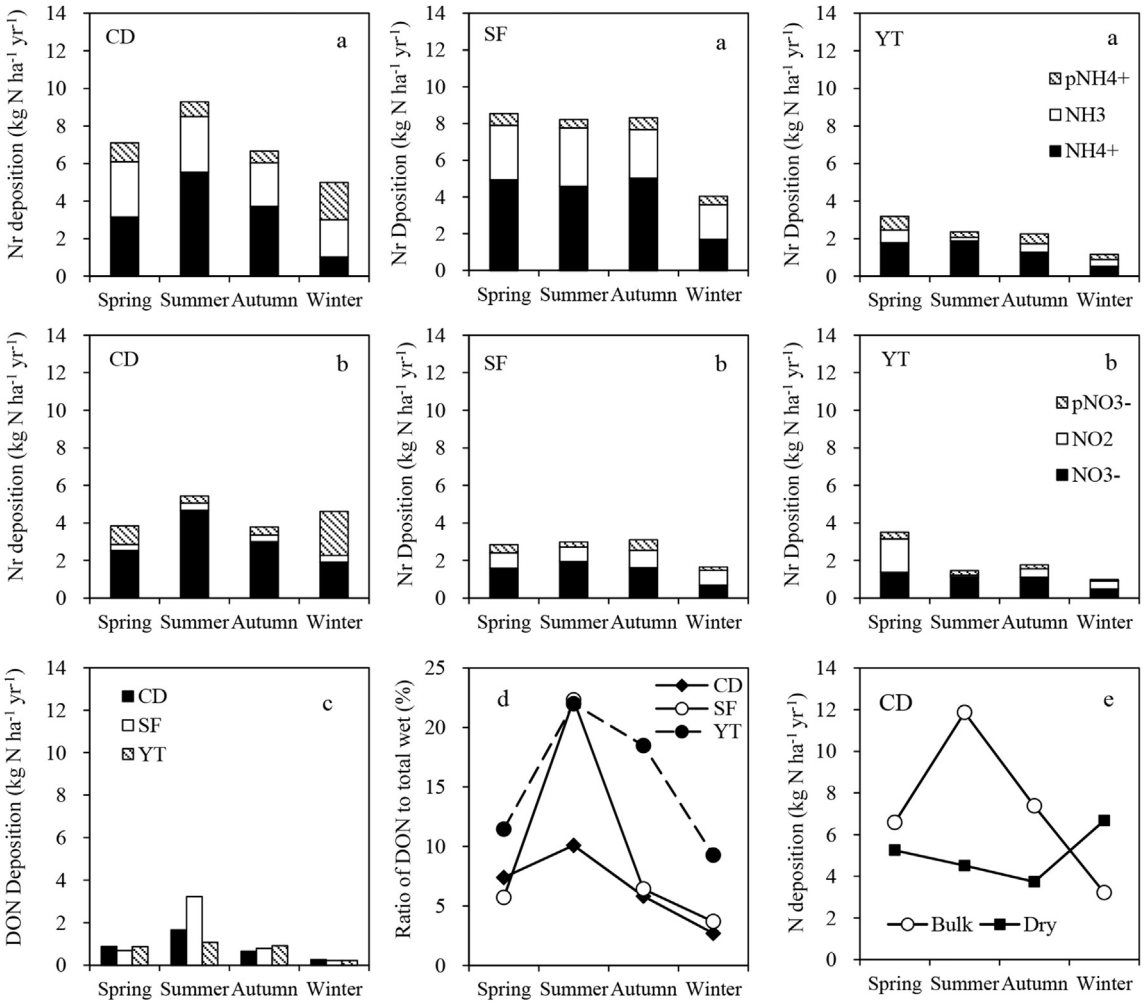

Fig. 5. Seasonal patterns for: (a) reduced N deposition rate (NH_4^+ in rainwater, gaseous NH_3 and aerosol pNH_4^+), (b) oxidized N deposition rate (NO_3^- in rainwater, gaseous NO_2 and aerosol pNO_3^-), (c) DON bulk deposition rate, (d) contribution of DON to total bulk deposition, and (e) the independent bulk and dry N deposition rates at CD.

Recent studies conducted in urban Beijing, North China found that waste and traffic may contribute with 50% to their total NH_3 emissions, of which more than 20% was emitted by traffic (Chang et al., 2016). Furthermore, NH_3 concentrations at all three study sites were significantly higher in summer than in winter due to the influence of air temperature on the partitioning between liquid phase NH_4^+ and gas phase NH_3 (Kurokawa et al., 2013). Every 5 °C temperature increase nearly doubles the volatilization potential of ammonia (Sutton et al., 2007). Ammonia is a highly soluble gas in water. It may react with H_2SO_4, leading to the formation of NH_4HSO_4 and $(NH_4)_2SO_4$, and the surplus NH_3 that does not react with H_2SO_4 will react with HNO_3, leading to the formation of NH_4NO_3 (Wang et al., 2005). The fact that higher pNH_4^+ concentrations were observed in winter compared with higher NH_3 in summer could be due to the lower winter temperatures favoring the transformation of NH_3 to pNH_4^+, especially as the precipitation scavenging effect in winter was weak due to low precipitation rates. The average NH_3 concentrations in the urban (CD) and suburban (SF) sites were comparable with that in North China (13.1 μg N m^{-3}), however, the NH_3 concentration at the agricultural site (YT) was lower than that in North China (16.9 μg N m^{-3}) (Xu et al., 2016). Furthermore, the NH_3 concentrations in the urban (CD) and suburban (SF) sites were comparable with global hotspots elsewhere. For example annual NH_3 concentrations at an urban measurement station in Delhi, India were estimated at 17.8 ± 3.4 μg N m^{-3} (Sharma et al., 2017).

By convention NO_2 concentrations reported in this and similar studies represent the wider group of nitrogen oxides, mainly NO and NO_2. Nitric oxide and NO_2 rapidly equilibrate in the presence of sunlight and the main source of NO are combustion processes (Kenty et al., 2007). Therefore it is not surprising that NO_2 concentrations at the agricultural site were significantly lower ($p < 0.01$) than in the urban and suburban sites and this is consistent with the spatial distribution pattern of emission sources in other regions of China (Xu et al., 2015). NO_2 concentrations were higher in the colder months and lower in the warmer months. This may be explained by the relatively higher boundary layer, shorter residence time and faster oxidation rate in warm periods leading to lower NO_2 concentrations (Fowler et al., 2009), and slower photochemical conversion and a shallow boundary layer height in winter would produce more NO_2 (Hargreaves et al., 2000). However, seasonal variability was not significant at all three study sites. Similar trends were also found in previous studies. For example, Wang et al. (2016) studied NO_2 concentrations in the urban site of Chengdu using $NO/NO_2/NO_x$ analyzer based on the chemiluminescence measurement principle and delivering hourly data. They also observed that seasonal NO_2 variations were not significant and smaller than a factor of 1.5. This differed from other studies in North

Please cite this article in press as: Song, L., et al., Ambient concentrations and deposition rates of selected reactive nitrogen species and their contribution to $PM_{2.5}$ aerosols at three locations with contrasting land use in southwest China, Environmental Pollution (2017), https://doi.org/10.1016/j.envpol.2017.10.002

China, which showed higher NO_2 concentrations in winter than in other periods due to coal combustion for domestic heating (Li et al., 2012). Unlike in the northern provinces of China, the climate in Sichuan province is relatively mild, and therefore the need for additional heating in winter is limited and avoids the large winter NO_2 emissions seen elsewhere. The seasonal pattern of NO_2 is also affected by the NO/NO_2 ratio. Supposing that NO_x concentrations are larger in winter, and there is an excess of NO compared to O_3, then the observed NO_2 seasonality would be muted (Han et al., 2011). Also situations where emission sources are close to the sampling location and transport time is less than the chemical lifetime of NO, will impact the seasonal pattern of NO_2 (Beirle et al., 2011). Therefore, we still need more studies to research the temporal changes of NO_2 emission and deposition rates. It has been reported that lower temperatures together with high NO_x emissions facilitate the formation of pNO_3^- (Mariani and de Mello, 2007). It is therefore likely that the significantly higher pNO_3^- concentrations in winter than in summer in the present study was mainly caused by the temperature differences and lower precipitation scavenging. Compared with other studies using passive samplers to study NO_2 concentration, the observed NO_2 concentrations were lower than in other developed regions of China. It was reported that the annual average NO_2 concentration can reach up to 42.2 μg N m^{-3} at the rural catchment in Jiangsu (Yang et al., 2010) and 39.5 μg N m^{-3} in the suburban of Beijing (Shen et al., 2009), which were twice the concentration at the urban site (CD) in our study. The values reported here were comparable with those observed at several urban sites in other Asia countries such as Nepal for which annual NO_2 concentrations was estimated at 22.4 ± 8.1 (Kiros et al., 2016). The NO_2 concentration at the agricultural site (YT) was even comparable with the background concentration of atmospheric NO_2 in North China (Meng et al., 2010).

4.2. Nr species deposition

Total N deposition rates estimated in the present study ranged from 19.8 to 49.2 kg N ha^{-1} yr^{-1}. The deposition rate in urban CD was comparable with that in North China, for which the total deposition rate was estimated to be 60.6 kg N ha^{-1} yr^{-1} with 60% as dry deposition (Pan et al., 2012). This implies that southwest China is experiencing Nr pollution levels similar to those in North China. Compared to previous measurements at CD (2008–2013), the precipitation in the present study was about 31.8% lower than in the 2008–2013 period and as a result the bulk deposition was about 23.6% lower than in our previous study (Song et al., 2017). As the continuous open bulk collectors may overestimate the actual wet deposition, this fraction was estimated at about 2.5% according to previous studies, which investigated N wet and bulk deposition simultaneously at the same agricultural site (YT) (Kuang et al., 2016; Song et al., 2017). According to Afshar-Mohajer et al. (2017) the overestimated fraction was mainly composed of coarse particulates.

Contributions of reduced N, oxidized N and DON to total N deposition (bulk plus dry deposition) were in the range of 53.2–66.1%, 24.4–36.7% and 6.5–14.8%, respectively. The reduced N dominated both bulk and dry deposition in the present study, indicating that reduced N plays a key role in N deposition in southwest China. Other studies conducted in other parts of China also found that reduced N dominated N deposition (Meng et al., 2010). However, the contribution of reduced N to bulk deposition has decreased from 80% in the 1980s to 55% in the early 2010s generally as a result of the increase in traffic and industrial activity in China (Xu et al., 2016). The highest proportion of oxidized N was found at the urban site (CD), and the highest proportion of DON was observed at the agricultural site (YT). This was consistent with previous research that relatively more traffic and industrial activity in an urban region will lead to more oxidized N emissions (Erisman et al., 2013) and that DON emissions were significantly influenced by agricultural activity (Cape et al., 2012). However, the proportion of reduced N in urban and suburban sites are also both high, and similar to the situation in Beijing, where both NH_3 and NO_2 concentrations decreased significantly after traffic reduction measures in Beijing during the 2015 China Victory Day Parade (Xu et al., 2017).

It should be noted that the estimated dry deposition in the present study has large uncertainties. Firstly, NH_3 fluxes over vegetated land are bi-directional, with differences between emission and deposition depending on environmental conditions, plant communities as well as other factors such as plant phenology (Sutton et al., 1998). Therefore, the compensation point approach was used to estimate NH_3 deposition fluxes over managed grassland and crops (Flechard et al., 2011). However, the compensation point was not considered in the present study, and NH_3 deposition fluxes may be overestimated at the agriculture and suburban sites which have relatively high canopy compensation points due to fertilized crops. Secondly, the contribution of other dry deposited N species, such as HNO_3, PM_{10} and organic N during our study period is unknown. However, N deposition flux ratios of HNO_3 to NH_3 were calculated from previous measurements at YT (2008–2013) and were 0.5, 0.2, 0.6 and 0.9, respectively in spring, summer, autumn and winter (Kuang et al., 2016). Since we did not have measurements of HNO_3 at CD and SF, we assumed these ratios to be similar, and inferred that HNO_3 deposition fluxes may contribute with 1.1, 0.5, 1.1, and 1.3 kg N ha^{-1} yr^{-1} in spring, summer, autumn and

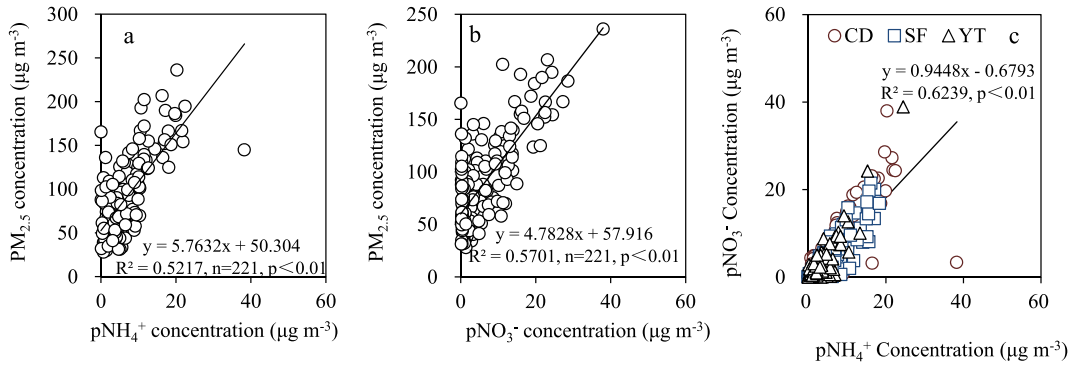

Fig. 6. Correlations for ambient $PM_{2.5}$ concentration with pNH_4^+ (a), pNO_3^- (b) at CD, and (c) the correlation between pNH_4^+ and pNO_3^- at CD, SF and YT during the monitoring period. Since the correlations for ambient $PM_{2.5}$ concentration with pNH_4^+ or pNO_3^- at three monitoring sites all showed significant positive relationship, we only show the data for CD as an example.

Please cite this article in press as: Song, L., et al., Ambient concentrations and deposition rates of selected reactive nitrogen species and their contribution to $PM_{2.5}$ aerosols at three locations with contrasting land use in southwest China, Environmental Pollution (2017), https://doi.org/10.1016/j.envpol.2017.10.002

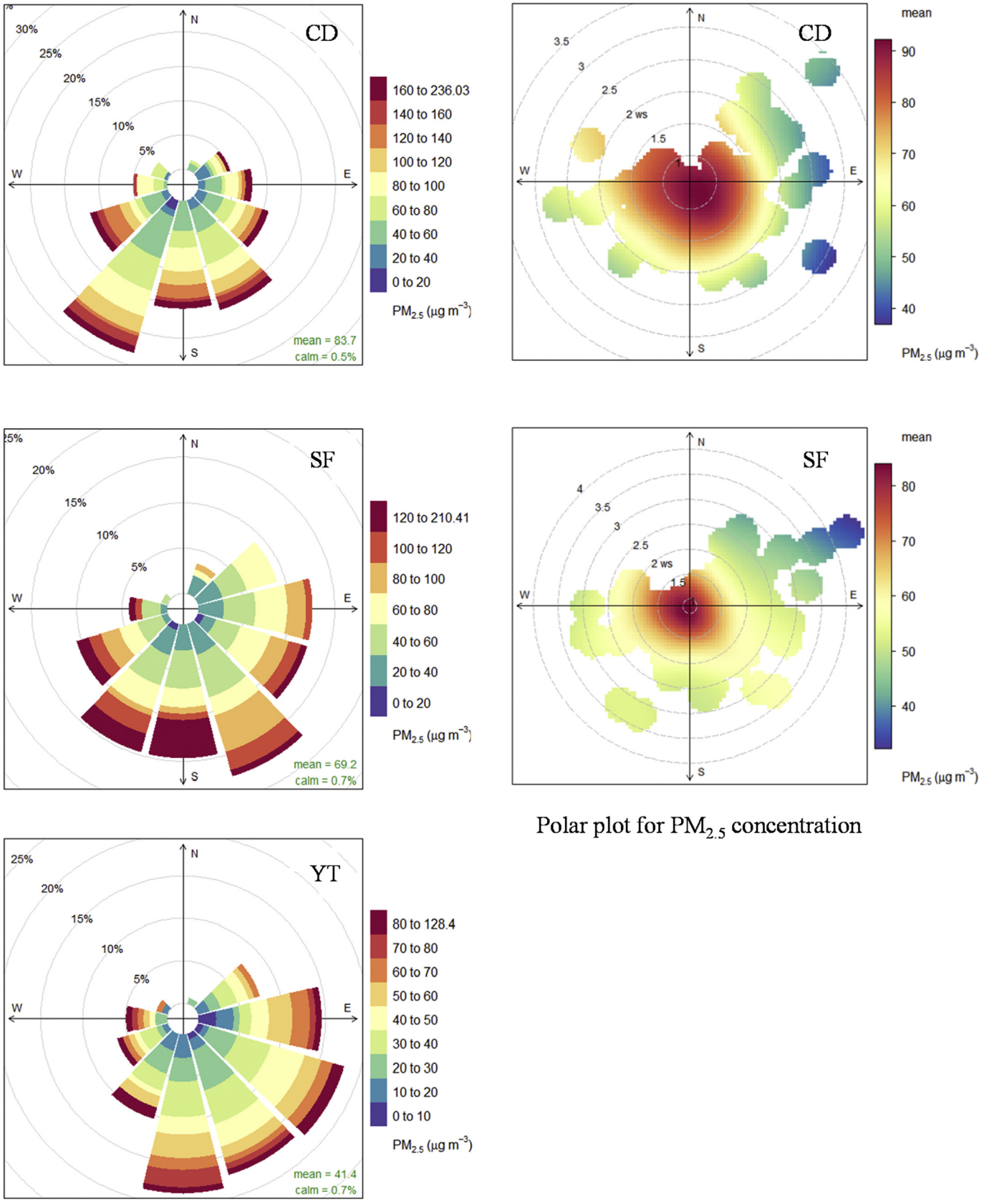

Fig. 7. Bivariate frequency distribution plots (left) and polar plots (right) of $PM_{2.5}$ concentrations during the monitoring period at the three monitoring sites. The center of each plot represents a wind frequency or wind speed of zero, which increased radially outward. The concentration of $PM_{2.5}$ is shown by the color scale (Graphs produced using Openair; Carslaw and Ropkins, 2012).

Please cite this article in press as: Song, L., et al., Ambient concentrations and deposition rates of selected reactive nitrogen species and their contribution to $PM_{2.5}$ aerosols at three locations with contrasting land use in southwest China, Environmental Pollution (2017), https://doi.org/10.1016/j.envpol.2017.10.002

winter, respectively. Not measuring HNO_3 may have led to an underestimate of the total N deposition rate at CD and SF by about 9%, 4%, 10% and 17%, respectively, in spring, summer, autumn and winter.

4.3. Source analysis for $PM_{2.5}$ pollution

Fine particles ($PM_{2.5}$) are a main societal concern in China because of their long atmospheric residence time, high surface to volume ratio, and high impact on human health, visibility, climate and on ecosystems (Tiwari et al., 2012). Annual average $PM_{2.5}$ concentrations were 83.4, 69.2 and 41.7 μg m^{-3} at the urban (CD), suburban (SF) and agriculture (YT) sites, respectively, which is comparable with similar studies conducted in North China (Xu et al., 2017), but much larger than measurements made in European and North American cities. According to the Chinese Grade II standard for $PM_{2.5}$ (75 μg m^{-3}) at more than 30% of sampling days, daily average $PM_{2.5}$ concentration exceeded this standard at CD and SF, but only 8% of the sampling days exceeded this standard at YT. However, comparing our data with the WHO standards for daily average $PM_{2.5}$ (25 μg m^{-3}), more than 95% of the sampling days exceeded this standard at CD and SF. And even at YT, more than 75% of sampling days exceeded this standard (Table 1).

$PM_{2.5}$ includes both primary and secondary sources, with both local and long range contributions. The secondary aerosols are closely coupled to chemical processing of primary pollutants in the atmosphere. Water-soluble ions, carbonaceous aerosols and surface derived insoluble compounds all contribute to the measured particulate matter (Gao et al., 2015). The $PM_{2.5}$ concentrations measured in this study showed similar seasonal variations with pNH_4^+ and pNO_3^-, which was lower in the rainy season and higher in the dry season (Fig. 4). The fine particulate NH_4^+ and NO_3^- contributed with 7.6% and 5.5%, respectively, on average to total $PM_{2.5}$ concentrations in our study (Table 1). The combination of NH_4^+ and NO_3^- as well as SO_4^{2-} may account for 80% of the water soluble inorganic ions in $PM_{2.5}$ in the present study (Table 1). The contribution of secondary inorganic aerosols to $PM_{2.5}$ was estimated to be 24.5–29.1% and this proportion was consistent with previous studies conducted in Chongqing, a mega city located near Sichuan province (He et al., 2012), indicating that secondary inorganic aerosols play an important role in increased $PM_{2.5}$ pollution in our study region. Concentrations of pNH_4^+ and pNO_3^- showed a significant ($p < 0.01$) positive relationship with $PM_{2.5}$ concentration (Fig. 6), with similar trends found at all three sites. Meanwhile, pNH_4^+ and pNO_3^- concentrations also showed significant ($p < 0.01$) linear correlation (Fig. 6).

The ratio of NO_3^-/SO_4^{2-} (0.4, 0.4 and 0.3 at CD, SF and YT, respectively) was lower than in other developed cities in North China where the ratio was in the range of 0.75–1.07 (Zhao et al., 2013). This difference may be attributed to regional differences in energy structure and meteorology. The lower NO_3^-/SO_4^{2-} could also further reflect the fact that the air pollution in our study area was more influenced by the coal consumption required by the manufacturing industry rather than by transport emissions. Furthermore, fine particulate Ca^{2+} and K^+ mainly originate from mineral dust and biomass burning, respectively (Zhao et al., 2010). The inconsistent trends of higher Ca^{2+} than K^+ concentrations at the urban site CD and higher K^+ than Ca^{2+} at the suburban site SF, and the agricultural site YT may be caused by different sources emitted from roads, soil dust and biomass burning. To further identify and understand the sources of the measured $PM_{2.5}$ concentrations, frequency and polar coordinates of $PM_{2.5}$ concentrations with wind direction and speed dependence were determined using the Openair software package (Fig. 7) (Carslaw and Ropkins, 2012). It was found that $PM_{2.5}$ concentrations were higher under lower wind speed and that pollutants in CD and SF were mainly from local emission sources. In CD, our monitoring site is located in the urban center near the 1st ring road, and most of the pollution sources came from south of Chengdu. This was consistent with the fact that the majority of the polluting activities were located to the south of the monitoring station, which was the more industrialized part of the city. In SF, our monitoring site is located to the northeast and 50 km away from CD, most of the pollutants were from local emissions while many of the pollutants and notably NO_2 also came from CD. At the agricultural site YT, NH_3 was emitted by local sources. The main source of NO_2 at YT is likely to be the mega city Chongqing, which is about 200 km away, rather than CD (Zheng et al., 2014). Integrated measures to reduce reactive N emission from agricultural activities, traffic and industrial sources are necessary to improve the air quality in southwest China.

5. Conclusions

Bulk and dry deposition of Nr, and $PM_{2.5}$ concentrations and composition were observed in urban (CD), suburban (SF) and agricultural (YT) sites in southwest China. The estimated total N deposition rates were in the range of 19.8–49.2 kg N ha^{-1} yr^{-1}. Reduced N, oxidized N and organic N (in bulk deposition) contributed 58.7%, 31.0%, 10.3%, respectively, to total N deposition. Ammonia was the main dry deposition component. Significantly higher concentrations of NH_3 were measured at CD and SF than at YT, due to a multitude of sources in the urban and suburban areas. NO_2 concentrations were lower in warmer than the colder months. Proportions of daily $PM_{2.5}$ concentrations exceeding the WHO standard for daily average $PM_{2.5}$ reached more than 95% at CD and SF, and more than 75% at YT, indicating serious air pollution in the study region. The components of $PM_{2.5}$ were similar at the three study sites, with secondary ions (SO_4^{2-}, NO_3^- and NH_4^+) contributing about 26.7% in total. Fine particulate NH_4^+ and NO_3^- showed significant correlation with $PM_{2.5}$ concentrations. Most of the $PM_{2.5}$ pollution was caused by local sources in CD and SF, while substantial regional sources of NO_2 contributed to oxidized N at the YT location. Our results suggest that reactive N emissions are substantial, if not dominant contributor to $PM_{2.5}$ pollution. The control of reactive N emissions especially for NH_3 would significantly improve air quality in southwest China.

Acknowledgements

This study was financially supported by the Natural Science Foundation of China (Grants No. 41301321, 41271321, 41371303), Major Science and Technology Program for Water Pollution Control and Treatment (2017ZX07101-001), the Chinese Academy of Sciences ('Light of West China' Program) and the CINAg project. We sincerely thank the staff at Yanting and Shifang experimental station for help with collecting and analyzing samples. Furthermore we wish to thank the Chinese Academy of Sciences ('Visiting Scholar' Project) for supporting a one year academic visitor placement at CEH for Dr Ling Song.

Appendix A. Supplementary data

Supplementary data related to this article can be found at https://doi.org/10.1016/j.envpol.2017.10.002.

References

Aas, W., Shao, M., Jin, L., Larssen, T., Zhao, D., Xiang, R., Zhang, J., Xiao, J., Duan, L., 2007. Air concentrations and wet deposition of major inorganic ions at five non-urban sites in China, 2001–2003. Atmos. Environ. 41, 1706–1716.

Please cite this article in press as: Song, L., et al., Ambient concentrations and deposition rates of selected reactive nitrogen species and their contribution to $PM_{2.5}$ aerosols at three locations with contrasting land use in southwest China, Environmental Pollution (2017), https://doi.org/10.1016/j.envpol.2017.10.002

Afshar-Mohajer, N., Godfrey, W.H., Rule, A.M., Matsui, E.C., Gordon, J., Koehler, K., 2017. A low-cost device for bulk sampling of airborne particulate matter: evaluation of an ionic charging device. Aerosol Air Qual. Res. 17, 1452–1462.

Beirle, S., Boersma, K.F., Platt, U., Lawrence, M.G., Wagner, T., 2011. Megacity emissions and lifetimes of nitrogen oxides probed from space. Science 333, 1737–1739.

Bisht, D.S., Srivastava, A.K., Joshi, H., Ram, K., Singh, N., Naja, M., Srivastava, M.K., Tiwari, S., 2017. Chemical characterization of rainwater at a high-altitude site "Nainital" in the central Himalayas, India. Environ. Sci. Pollut. Res. 24, 3959–3969.

Bronk, D.A., Lomas, M.W., Glibert, P.M., Schukert, K.J., Sanderson, M.P., 2000. Total dissolved nitrogen analysis: comparisons between the persulfate, UV and high temperature oxidation methods. Mar. Chem. 69, 163–178.

Bush, T., Smith, S., Stevenson, K., Moorcroft, S., 2001. Validation of nitrogen dioxide diffusion tube methodology in the UK. Atmos. Environ. 35, 289–296.

Cape, J.N., Leith, I.D., 2002. The contribution of dry deposited ammonia and sulphur dioxide to the composition of precipitation from continuously open gauges. Atmos. Environ. 36, 5983–5992.

Cape, J.N., Tang, Y.S., Gonzalez-Benitez, J.M., Mitosinkova, M., Makkonen, U., Jocher, M., Stolk, A., 2012. Organic nitrogen in precipitation across Europe. Biogeosciences 9, 4401–4409.

Carslaw, D.C., Ropkins, K., 2012. Openair — an R package for air quality data analysis. Environ. Model. Softw. 27–28, 52–61.

Chang, Y., Liu, X., Deng, C., Dore, A.J., Zhuang, G., 2016. Source apportionment of atmospheric ammonia before, during, and after the 2014 APEC summit in Beijing using stable nitrogen isotope signatures. Atmos. Chem. Phys. 16, 11635–11647.

Delon, C., Galy-Lacaux, C., Adon, M., Liousse, C., Serça, D., Diop, B., Akpo, A., 2012. Nitrogen compounds emission and deposition in West African ecosystems: comparison between wet and dry savanna. Biogeosciences 9, 385–402.

Dore, A.J., Carslaw, D.C., Braban, C., Cain, M., Chemel, C., Conolly, C., Derwent, R.G., Griffiths, S.J., Hall, J., Hayman, G., Lawrence, S., Metcalfe, S.E., Redington, A., Simpson, D., Sutton, M.A., Sutton, P., Tang, Y.S., Vieno, M., Werner, M., Whyatt, J.D., 2015. Evaluation of the performance of different atmospheric chemical transport models and inter-comparison of nitrogen and sulphur deposition estimates for the UK. Atmos. Environ. 119, 131–143.

Erisman, J.W., Galloway, J.N., Seitzinger, S., Bleeker, A., Dise, N.B., Petrescu, A.M.R., Leach, A.M., de Vries, W., 2013. Consequences of human modification of the global nitrogen cycle. Philosophical Trans. R. Soc. B-Biological Sci. 368 https://doi.org/10.1098/rstb.2013.0116.

Feng, X.Q., Wang, X.R., He, M., Han, L., 2015. A 2012-based anthropogenic ammonia emission inventory and its spatial distribution in Sichuan Province[J]. Acta Sci. Circumstantiae 35, 394–401 (In Chinese with English abstract).

Flechard, C.R., Nemitz, E., Smith, R.I., Fowler, D., Vermeulen, A.T., Bleeker, A., Erisman, J.W., Simpson, D., Zhang, L., Tang, Y.S., Sutton, M.A., 2011. Dry deposition of reactive nitrogen to European ecosystems: a comparison of inferential models across the NitroEurope network. Atmos. Chem. Phys. 11, 2703–2728.

Fowler, D., Pilegaard, K., Sutton, M.A., Ambus, P., Raivonen, M., Duyzer, J., Simpson, D., Fagerli, H., Fuzzi, S., Schjoerring, J.K., Granier, C., Neftel, A., Isaksen, I.S.A., Laj, P., Maione, M., Monks, P.S., Burkhardt, J., Daemmgen, U., Neirynck, J., Personne, E., Wichink-Kruit, R., Butterbach-Bahl, K., Flechard, C., Tuovinen, J.P., Coyle, M., Gerosa, G., Loubet, B., Altimir, N., Gruenhage, L., Ammann, C., Cieslik, S., Paoletti, E., Mikkelsen, T.N., Ro-Poulsen, H., Cellier, P., Cape, J.N., Horvath, L., Loreto, F., Niinemets, U., Palmer, P.I., Rinne, J., Misztal, P., Nemitz, E., Nilsson, D., Pryor, S., Gallagher, M.W., Vesala, T., Skiba, U., Brueggemann, N., Zechmeister-Boltenstern, S., Williams, J., O'Dowd, C., Facchini, M.C., de Leeuw, G., Flossman, A., Chaumerliac, N., Erisman, J.W., 2009. Atmospheric composition change: ecosystems-Atmosphere interactions. Atmos. Environ. 43, 5193–5267.

Fowler, D., Steadman, C.E., Stevenson, D., Coyle, M., Rees, R.M., Skiba, U.M., Sutton, M.A., Cape, J.N., Dore, A.J., Vieno, M., Simpson, D., Zaehle, S., Stocker, B.D., Rinaldi, M., Facchini, M.C., Flechard, C.R., Nemitz, E., Twigg, M., Erisman, J.W., Butterbach-Bahl, K., Galloway, J.N., 2015. Effects of global change during the 21st century onthe nitrogen cycle. Atmos. Chem. Phys. 15, 13849–13893.

Gao, J., Tian, H., Cheng, K., Lu, L., Zheng, M., Wang, S., Hao, J., Wang, K., Hua, S., Zhu, C., Wang, Y., 2015. The variation of chemical characteristics of PM2.5 and PM10 and formation causes during two haze pollution events in urban Beijing, China. Atmos. Environ. 107, 1–8.

Han, S., Bian, H., Feng, Y., Liu, A., Li, X., Zeng, F., Zhang, X., 2011. Analysis of the relationship between O-3, NO and NO2 in Tianjin, China. Aerosol Air Qual. Res. 11, 128–139.

Hargreaves, P.R., Leidi, A., Grubb, H.J., Howe, M.T., Mugglestone, M.A., 2000. Local and seasonal variations in atmospheric nitrogen dioxide levels at Rothamsted, UK, and relationships with meteorological conditions. Atmos. Environ. 34, 843–853.

He, K., Zhao, Q., Ma, Y., Duan, F., Yang, F., Shi, Z., Chen, G., 2012. Spatial and seasonal variability of PM2.5 acidity at two Chinese megacities: insights into the formation of secondary inorganic aerosols. Atmos. Chem. Phys. 12, 1377–1395.

Huang, J., Zhang, W., Zhu, X., Gilliam, F.S., Chen, H., Lu, X., Mo, J., 2015. Urbanization in China changes the composition and main sources of wet inorganic nitrogen deposition. Environ. Sci. Pollut. Res. 22, 6526–6534.

Ianniello, A., Spataro, F., Esposito, G., Allegrini, I., Hu, M., Zhu, T., 2011. Chemical characteristics of inorganic ammonium salts in PM2.5 in the atmosphere of Beijing (China). Atmos. Chem. Phys. 11, 10803–10822.

Kenty, K.L., Poor, N.D., Kronmiller, K.G., McClenny, W., King, C., Atkeson, T., Campbell, S.W., 2007. Application of CALINE4 to roadside NO/NO2 transformations. Atmos. Environ. 41, 4270–4280.

Kiros, F., Shakya, K.M., Rupakheti, M., Regmi, R.P., Maharjan, R., Byanju, R.M., Naja, M., Mahata, K., Kathayat, B., Peltier, R.E., 2016. Variability of anthropogenic gases: nitrogen oxides, sulfur dioxide, ozone and ammonia in Kathmandu valley, Nepal. Aerosol Air Qual. Res. 16, 3088–3101.

Kuang, F., Liu, X., Zhu, B., Shen, J., Pan, Y., Su, M., Goulding, K., 2016. Wet and dry nitrogen deposition in the central Sichuan Basin of China. Atmos. Environ. 143, 39–50.

Kurokawa, J., Ohara, T., Morikawa, T., Hanayama, S., Janssens-Maenhout, G., Fukui, T., Kawashima, K., Akimoto, H., 2013. Emissions of air pollutants and greenhouse gases over Asian regions during 2000–2008: regional Emission inventory in ASia (REAS) version 2. Atmos. Chem. Phys. 13, 11019–11058.

Lee, H.M., Paulot, F., Henze, D.K., Travis, K., Jacob, D.J., Pardo, L.H., Schichtel, B.A., 2016. Sources of nitrogen deposition in Federal Class I areas in the US. Atmos. Chem. Phys. 16, 525–540.

Li, K.H., Song, W., Liu, X.J., Shen, J.L., Luo, X.S., Sui, X.Q., Liu, B., Hu, Y.K., Christie, P., Tian, C.Y., 2012. Atmospheric reactive nitrogen concentrations at ten sites with contrasting land use in an arid region of central Asia. Biogeosciences 9, 4013–4021.

Liu, X., Zhang, Y., Han, W., Tang, A., Shen, J., Cui, Z., Vitousek, P., Erisman, J.W., Goulding, K., Christie, P., Fangmeier, A., Zhang, F., 2013. Enhanced nitrogen deposition over China. Nature 494, 459–462.

Mariani, R.L., de Mello, W.Z., 2007. PM2.5–10, PM2.5 and associated water-soluble inorganic species at a coastal urban site in the metropolitan region of Rio de Janeiro. Atmos. Environ. 41, 2887–2892.

Meng, Z.Y., Xu, X.B., Wang, T., Zhang, X.Y., Yu, X.L., Wang, S.F., Lin, W.L., Chen, Y.Z., Jiang, Y.A., An, X.Q., 2010. Ambient sulfur dioxide, nitrogen dioxide, and ammonia at ten background and rural sites in China during 2007–2008. Atmos. Environ. 44, 2625–2631.

Meng, Z.Y., Lin, W.L., Jiang, X.M., Yan, P., Wang, Y., Zhang, Y.M., Jia, X.F., Yu, X.L., 2011. Characteristics of atmospheric ammonia over Beijing, China. Atmos. Chem. Phys. 11, 6139–6151.

Ozden, O., Dogeroglu, T., 2008. Field evaluation of a tailor-made new passive sampler for the determination of NO2 levels in ambient air. Environ. Monit. Assess. 142, 243–253.

Pan, Y.P., Wang, Y.S., Tang, G.Q., Wu, D., 2012. Wet and dry deposition of atmospheric nitrogen at ten sites in Northern China. Atmos. Chem. Phys. 12, 6515–6535.

Petroff, A., Zhang, L., 2010. Development and validation of a size-resolved particle dry deposition scheme for application in aerosol transport models. Geosci. Model Dev. 3, 753–769.

Puchalski, M.A., Sather, M.E., Walker, J.T., Lelunann, C.M.B., Gay, D.A., Mathew, J., Robargef, W.P., 2011. Passive ammonia monitoring in the United States: comparing three different sampling devices. J. Environ. Monit. 13, 3156–3167.

Rowland, A.P., Haygarth, P.M., 1997. Determination of total dissolved phosphorus in soil solutions. J. Environ. Qual. 26, 410–415.

Sanz-Cobena, A., Lassaletta, L., Estellés, F., Del Prado, A., Guardia, G., Abalos, D., Aguilera, E., Pardo, G., Vallejo, A., Sutton, M.A., Garnier, J., Billen, G., 2014. Yield-scaled mitigation of ammonia emission from N fertilization: the Spanish case. Environ. Res. Lett. 9, 125005.

Sharma, S.K., Saraswati, Mandal, T.K., Saxena, M., 2017. Inter-annual variation of ambient ammonia and related trace gases in Delhi, India. Bull. Environ. Contam. Toxicol. https://doi.org/10.1007/s00128-017-2058-x.

Shen, J., Chen, D., Bai, M., Sun, J., Coates, T., Lam, S.K., Li, Y., 2016. Ammonia deposition in the neighbourhood of an intensive cattle feedlot in Victoria, Australia. Sci. Rep. 6, 32793. https://doi.org/10.1038/srep32793.

Shen, J.L., Tang, A.H., Liu, X.J., Fangmeier, A., Goulding, K.T.W., Zhang, F.S., 2009. High concentrations and dry deposition of reactive nitrogen species at two sites in the North China Plain. Environ. Pollut. 157, 3106–3113.

Song, L., Kuang, F., Skiba, U., Zhu, B., Liu, X., Levy, P., Dore, A., Fowler, D., 2017. Bulk deposition of organic and inorganic nitrogen in southwest China from 2008 to 2013. Environ. Pollut. 227, 157–166.

Squizzato, S., Masiol, M., Brunelli, A., Pistollato, S., Tarabotti, E., Rampazzo, G., Pavoni, B., 2013. Factors determining the formation of secondary inorganic aerosol: a case study in the Po Valley (Italy). Atmos. Chem. Phys. 13, 1927–1939.

Stevens, C.J., Dise, N.B., Mountford, J.O., Gowing, D.J., 2004. Impact of nitrogen deposition on the species richness of grasslands. Science 303, 1876–1879.

Suarez-Bertoa, R., Zardini, A.A., Astorga, C., 2014. Ammonia exhaust emissions from spark ignition vehicles over the New European Driving Cycle. Atmos. Environ. 97, 43–53.

Sutton, M.A., Burkhardt, J.K., Guerin, D., Nemitz, E., Fowler, D., 1998. Development of resistance models to describe measurements of bi-directional ammonia surface–atmosphere exchange. Atmos. Environ. 32, 473–480.

Sutton, M.A., Dragosits, U., Tang, Y.S., Fowler, D., 2000. Ammonia emissions from non-agricultural sources in the UK. Atmos. Environ. 34, 855–869.

Sutton, M.A., Nemitz, E., Erisman, J.W., Beier, C., Bahl, K.B., Cellier, P., de Vries, W., Cotrufo, F., Skiba, U., Di Marco, C., Jones, S., Laville, P., Soussana, J.F., Loubet, B., Twigg, M., Famulari, D., Whitehead, J., Gallagher, M.W., Neftel, A., Flechard, C.R., Herrmann, B., Calanca, P.L., Schjoerring, J.K., Daemmgen, U., Horvath, L., Tang, Y.S., Emmett, B.A., Tietema, A., Peñuelas, J., Kesik, M., Brueggemann, N., Pilegaard, K., Vesala, T., Campbell, C.L., Olesen, J.E., Dragosits, U., Theobald, M.R., Levy, P., Mobbs, D.C., Milne, R., Viovy, N., Vuichard, N., Smith, J.U., Smith, P., Bergamaschi, P., Fowler, D., Reis, S., 2007. Challenges in quantifying

Please cite this article in press as: Song, L., et al., Ambient concentrations and deposition rates of selected reactive nitrogen species and their contribution to $PM_{2.5}$ aerosols at three locations with contrasting land use in southwest China, Environmental Pollution (2017), https://doi.org/10.1016/j.envpol.2017.10.002

biosphere–atmosphere exchange of nitrogen species. Environ. Pollut. 150, 125–139.
Tang, Y.S., Cape, J.N., Sutton, M.A., 2001. Development and types of passive samplers for monitoring atmospheric NO2 and NH3 concentrations. Sci. World J. 1, 513–529.
Tiwari, S., Chate, D.M., Srivastava, A.K., Bisht, D.S., Padmanabhamurty, B., 2012. Assessments of PM1, PM2.5 and PM10 concentrations in Delhi at different mean cycles. Geofizika 29, 125–141.
Vet, R., Artz, R.S., Carou, S., Shaw, M., Ro, C.U., Aas, W., Baker, A., Bowersox, V.C., Dentener, F., Galy-Lacaux, C., Hou, A., Pienaar, J.J., Gillett, R., Forti, M.C., Gromov, S., Hara, H., Khodzher, T., Mahowald, N.M., Nickovic, S., Rao, P.S.P., Reid, N.W., 2014. A global assessment of precipitation chemistry and deposition of sulfur, nitrogen, sea salt, base cations, organic acids, acidity and pH, and phosphorus. Atmos. Environ. 93, 3–100.
Wang, H., Yang, F., Shi, G., Tian, M., Zhang, L., Zhang, L., Fu, C., 2016. Ambient concentration and dry deposition of major inorganic nitrogen species at two urban sites in Sichuan Basin, China. Environ. Pollut. 219, 235–244.
Wang, S.S., Nan, J.L., Shi, C.Z., Fu, Q.Y., Gao, S., Wang, D.F., Cui, H.X., Saiz-Lopez, A., Zhou, B., 2015a. Atmospheric ammonia and its impacts on regional air quality over the megacity of Shanghai, China. Sci. Rep. 5, 15842.
Wang, Y., Zhuang, G., Tang, A., Yuan, H., Sun, Y., Chen, S., Zheng, A., 2005. The ion chemistry and the source of PM 2.5 aerosol in Beijing. Atmos. Environ. 39, 3771–3784.
Wang, Z., Pan, L., Li, Y., Zhang, D., Ma, J., Sun, F., Xu, W., Wang, X., 2015b. Assessment of air quality benefits from the national pollution control policy of thermal power plants in China: a numerical simulation. Atmos. Environ. 106, 288–304.
Wesely, M.L., Hicks, B.B., 1977. Some factors that affect deposition rates of sulfur-dioxide and similar gases on vegetation. J. Air Pollut. Control Assoc. 27, 1110–1116.
Xu, W., Luo, X.S., Pan, Y.P., Zhang, L., Tang, A.H., Shen, J.L., Zhang, Y., Li, K.H., Wu, Q.H., Yang, D.W., Zhang, Y.Y., Xue, J., Li, W.Q., Li, Q.Q., Tang, L., Lu, S.H., Liang, T., Tong, Y.A., Liu, P., Zhang, Q., Xiong, Z.Q., Shi, X.J., Wu, L.H., Shi, W.Q., Tian, K., Zhong, X.H., Shi, K., Tang, Q.Y., Zhang, L.J., Huang, J.L., He, C.E., Kuang, F.H., Zhu, B., Liu, H., Jin, X., Xin, Y.J., Shi, X.K., Du, E.Z., Dore, A.J., Tang, S., Collett, J.L., Goulding, K., Sun, Y.X., Ren, J., Zhang, F.S., Liu, X.J., 2015. Quantifying atmospheric nitrogen deposition through a nationwide monitoring network across China. Atmos. Chem. Phys. 15, 12345–12360.
Xu, W., Song, W., Zhang, Y., Liu, X., Zhang, L., Zhao, Y., Liu, D., Tang, A., Yang, D., Wang, D., 2017. Air quality improvement in a megacity: implications from 2015 Beijing Parade Blue pollution control actions. Atmos. Chem. Phys. 17, 31–46.
Xu, W., Wu, Q., Liu, X., Tang, A., Dore, A.J., Heal, M.R., 2016. Characteristics of ammonia, acid gases, and PM2.5 for three typical land-use types in the North China Plain. Environ. Sci. Pollut. Res. 23, 1158–1172.
Yang, R., Hayashi, K., Zhu, B., Li, F., Yan, X., 2010. Atmospheric NH3 and NO2 concentration and nitrogen deposition in an agricultural catchment of Eastern China. Sci. Total Environ. 408, 4624–4632.
Zbieranowski, A.L., Aherne, J., 2013. Ambient concentrations of atmospheric ammonia, nitrogen dioxide and nitric acid in an intensive agricultural region. Atmos. Environ. 70, 289–299.
Zhang, J., Smith, K.R., 2007. Household air pollution from coal and biomass fuels in China: measurements, health impacts, and interventions. Environ. Health Perspect. 115, 848–855.
Zhang, L., Vet, R., Wiebe, A., Mihele, C., Sukloff, B., Chan, E., Moran, M.D., Iqbal, S., 2008. Characterization of the size-segregated water-soluble inorganic ions at eight Canadian rural sites. Atmos. Chem. Phys. 8, 7133–7151.
Zhang, L.M., Gong, S.L., Padro, J., Barrie, L., 2001. A size-segregated particle dry deposition scheme for an atmospheric aerosol module. Atmos. Environ. 35, 549–560.
Zhang, X.Y., Wang, Y.Q., Niu, T., Zhang, X.C., Gong, S.L., Zhang, Y.M., Sun, J.Y., 2012. Atmospheric aerosol compositions in China: spatial/temporal variability, chemical signature, regional haze distribution and comparisons with global aerosols. Atmos. Chem. Phys. 12, 779–799.
Zhang, Y., Wei, J., Tang, A., Zheng, A., Shao, Z., Liu, X., 2017. Chemical characteristics of PM2.5 during 2015 spring festival in Beijing, China. Aerosol Air Qual. Res. 17, 1169–1180.
Zhao, P.S., Dong, F., He, D., Zhao, X.J., Zhang, X.L., Zhang, W.Z., Yao, Q., Liu, H.Y., 2013. Characteristics of concentrations and chemical compositions for PM2.5 in the region of Beijing, Tianjin, and Hebei, China. Atmos. Chem. Phys. 13, 4631–4644.
Zhao, Q., He, K., Rahn, K.A., Ma, Y., Jia, Y., Yang, F., Duan, F., Lei, Y., Chen, G., Cheng, Y., Liu, H., Wang, S., 2010. Dust storms come to Central and Southwestern China, too: implications from a major dust event in Chongqing. Atmos. Chem. Phys. 10, 2615–2630.
Zheng, B., Huo, H., Zhang, Q., Yao, Z., Wang, X., Yang, X., Liu, H., He, K., 2014. High-resolution mapping of vehicle emissions in China in 2008. Atmos. Chem. Phys. 14, 9787–9805.
Zhu, B., Wang, T., Kuang, F., Luo, Z., Tang, J., Xu, T., 2009. Measurements of nitrate leaching from a hillslope cropland in the central Sichuan basin, China. Soil Sci. Soc. Am. J. 73, 1419–1426.
Zimmermann, F., Lux, H., Maenhaut, W., Matschullat, J., Plessow, K., Reuter, F., Wienhaus, O., 2003. A review of air pollution and atmospheric deposition dynamics in southern Saxony, Germany, Central Europe. Atmos. Environ. 37, 671–691.

Please cite this article in press as: Song, L., et al., Ambient concentrations and deposition rates of selected reactive nitrogen species and their contribution to $PM_{2.5}$ aerosols at three locations with contrasting land use in southwest China, Environmental Pollution (2017), https://doi.org/10.1016/j.envpol.2017.10.002